NOTICE CONCERNING COPYRIGHT RESTRICTIONS

2D Finite Element Modelling of Regional and Local Fracture Networks in the Eastern California Shear Zone and Coso Range, California USA

Andreas Eckert and Peter Connolly

Geophysical Institute, University of Karlsruhe

Keywords

Coso, Sierra Nevada, transtension, bend, finite element, fracture potential

ABSTRACT

Geothermal energy production from the Coso field, located in the Eastern Californian Shear Zone, is reliant on a thorough understanding of the fluid flow network, which is controlled by the distribution and interaction of fractures and permeability. This paper presents the results of 2D linear elastic finite element (FE) modelling investigating the influence boundary conditions on the deformation field across the Coso Range, California. Loads equivalent to the motion of the main tectonic elements and internal fault slips yield results that compare favourably to published strain orientations and natural seismicity. Comparison of predicted shear fractures, generated using fracture potential, to seismicity shows that fracture reactivation, rather intact rock failure, is the most active brittle process. The numerical results support the concept that transtension in the Eastern California Shear Zone is driven by the relative NW motion of the Sierra Nevada Block.

Introduction

The Coso geothermal system is the largest geothermal field in the U.S. Basin and Range province, producing up to 240MWe from fractured rocks. Improved exploitation of the field is sought by a better understanding of the fracture networks controlling the sub-surface fluid flow. The Coso Range has recently been re-interpreted as being situated within a releasing bend structure that transfers dextral slip from the Airport Lake Fault Zone (ALFZ) to the Owens Valley Fault (OVF; Unruh et al., 2002). Second order faulting is a key control on fluid flow within transtensional bends (Connolly & Cosgrove, 1999). 2D map view finite element (FE) models are used to investigate the location, distribution, orientation and relative likelihood of different fracture types (tensile or shear) associated with the releasing bend structure. The FE results are correlated to strain orientations and seismicity catalogues. The best-fit model results provide an improved understanding of regional tectonics, fracture processes in the Coso Range/Coso Geothermal Field and are used as input for new, 3D, FE models of the region (Eckert & Connolly, in-prep).

Tectonic Setting of the Coso Range-Indian Wells Valley Region

The Eastern California Shear Zone (ECSZ) accommodates up to ~25% (~12mm/yr dextral shear) of the relative motion between the North American plate and the Pacific plate (Figure1a; Dokka & Travis, 1990). North of the Garlock Fault, the ECSZ is mainly expressed by three major right lateral fault zones: the Death Valley-Furnace Creek, the Hunter Mountain-Panamint Valley and Owens Valley-Airport Lake structures (Figure1a; Bennett et al., 1997). The Coso Range-Indian Wells Valley region is located within the Owens Valley – Airport Lake Fault Zone and is an area of both tectonic and volcanic activity bounded to the east by the Basin and Range province (Dokka & Travis, 1990). To the west, the Coso Range-Indian Wells Valley region is bounded by the NW moving Sierra Nevada Block (Dixon et. al., 2000). To the south, the Garlock Fault separates the Coso Range-Indian Wells Valley region from the Mojave Block.

Analysis of GPS velocity fields (McClusky et al., 2001) indicates that half of the shear in the ECSZ is accommodated on the ALFZ and the OVF, located south and north of the Coso Range respectively. The northward extension of the ALFZ steps eastward (~5km) via the Coso Wash Fault (CWF) and Haiwee Springs Fault Zone (HSFZ) structures to become the Owens Valley Fault. Unruh et al. (2002) conclude that shear transfer on this entire fault system forms a dilational step-over that drives crustal extension in the Coso Range. Unruh et al. (2002) also suggest that the bulk transtension of the Indian Wells Valley-Coso Range arises because the region is attached to the NW moving Sierra Nevada and that the fault zone represents the tectonic boundary of the Sierra Nevada Block.

Three-dimensional analogue and preliminary 2D FE models suggested that the ALFZ, CWF, HSFZ and OVF structures are linked at depth to form a bend rather than a step (Dooley & McClay, 2003). Analysis of contemporary stress data and the orientation of maximum extensional strain rate (N73°W) for the ECSZ indicates active northeast-southwest compressional and northwest-southeast extensional deformation across the Coso Range (Roquemore, 1980, Walter & Weaver, 1980, Feng & Lees, 1998; Gan et al., 2000; Monastero et al., 2002; Unruh et al., 2002). The stress and strain data support hypothesis of a current dextral transtensional stress regime in the ECSZ.

The Coso Geothermal Field (CGF) is located on the CWF, in a region of fumaroles, hot springs and steaming fissures along a series of left-stepping en-echelon fault segments of a negative flower structure (Figure1b).

Finite Element (FE) Model Definition

In order to predict fractures at a local scale (<1km) it is necessary to account for the larger scale tectonics. The 2D map-view model area was selected based on the ECSZ fault pattern (Fig.1a) and includes the SW Basin and Range, the northern ECSZ and southern Sierra Nevada tectonic regimes (Figure1c). The loading effects of these regimes, together with the active fault slips, are modelled using the commercial FE code ABAQUS™. In order to study the stress state in the smaller region of the inferred bend passing through Coso (Figure1b) the ABAQUS sub-modelling technique is used (ABAQUS users manual). The Coso sub-model comprises all the major faults (ALFZ, LLF and the bend structure) as well as most of the known second order structures (Figure1d).

Granitic plutons are the dominant lithology in the study area (Duffied et al., 1980). Hence, the FE model utilizes a homogeneous, linear elastic material with Young's modulus, E, of 70GPa and Poison's Ratio, ν, of 0.3 (Landolt-Börnstein, 1982). The surface mapped fault traces are included as frictional contact surfaces with a coefficient of friction, μ, typical for brittle upper crust (0.6; Turcotte & Schubert, 2002).

Loading Conditions

Detailed studies of the tectonic loading, loading period and relative motion of the Sierra Nevada Block were undertaken in order to ascertain the best combination of loading conditions to fit the tectonic regime, strain orientations and seismicity acting on the ECSZ and Coso Range. The motions of the various tectonic blocks, inferred from GPS measurements, are applied as the external loads to the global model. The sub-model is driven externally by interpolation of the global model results.

In both the global and sub-model cases, internal loading that is equivalent to the GPS determined slip rates is applied parallel to each fault segment. All modelled second order faults are part of either the Airport Lake Fault Zone or the bend structure and exhibit dextral oblique slip. The second order faults are assigned 40% of the measured slip to mimic only the map-view, pure-dex-

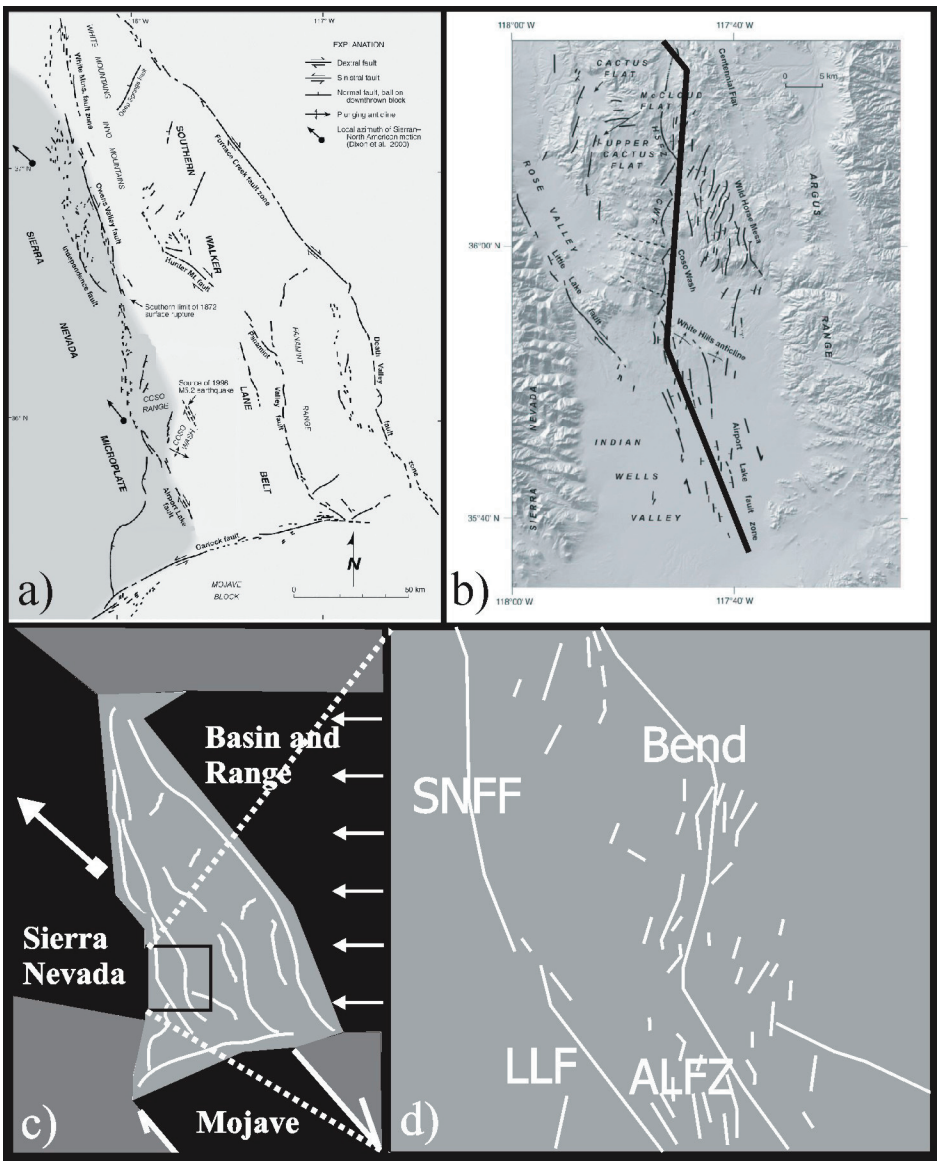

Figure 1.

a) Map of the Quaternary active fault distribution in East California Shear Zone (from Unruh et al. 2002).

b) Active fault map of the Coso Range-Indian Wells Valley region. Solid black line indicates the trace of the inferred bend structure transferring shear from the Airport Lake Fault Zone to the Owens Valley Fault (after Unruh et al. 2002).

c) Geometry and external boundary conditions applied to the global finite element model. Trace of the modelled faults follow those of (a).

d) Fault geometry used for the submodel.

tral slip, component. Dip-slip faults, such as the extensional Wilson Canyon and Sierra Nevada Frontal faults, have zero slip assigned.

To simulate temporal stress increase, the FE models are run over five different periods: 1 year, 10, 50, 100, and 1000 years by linearly extrapolating the known 1 year fault slips to the appropriate time step.

Derivation of Fracture Predictions From Stress Data: The Fracture Potential (FP) Method

The type of fractures generated/reactivated is critical in understanding fluid flow in the Coso Geothermal Field and, therefore, a distinction between tensile and shear fractures must be made in the analysis of the FE results. The likelihood of fracture generation/reactivation due to the local stress state must also be considered. The concept of fracture potential (FP; Connolly, 1996) enables both of these distinctions to be made and is utilized herein. This is based on the combined Griffith/Navier-Coulomb failure criterion (Jaeger & Cook, 1969; Price & Cosgrove, 1990)

In the tensile regime (when differential stress, σ_d, is less than 4T) the tensile-FP (tFP) magnitude is the ratio of σ_3 to the tensile strength, T, of the material (Figure 2a):

$$tFP = \frac{\sigma_3}{T} \quad (1)$$

In the shear regime (σ_d is greater than 4T) the shear-FP (sFP) is defined by the relationship between the critical differential stress at failure $\sigma_{d,crit}$ and the differential stress σ_d (Figure 2b):

$$sFP = \frac{\sigma_d/2}{\sigma_{d,crit}/2} = \frac{\sigma_d}{2\left(c_0 \cos\phi + \sigma_m \sin\phi\right)} \quad (2)$$

The sFP is only determined if $\sigma_d > 4T$. When $\sigma_d < 4T$ and $\sigma_3 > 0$ a compressional state of stress must exist and tensile failure cannot occur. In this situation, FP is assigned 0. Sign convention is such that at tensile failure, tFP = –1 and at shear failure, sFP = +1.

In this study sFP and tFP are calculated for the local state of stress at each integration (data) point within the model. The FP results are used, in combination with possible fracture orientations, to predict the likely fracture network. Tensile fractures are predicted to form normal to the local minimum principal stress and shear fractures at 45 ± $\tan^{-1}\mu$ to the maximum principal stress orientation.

Application of Fracture Potential (FP) to 2D Finite Element Results

Seven idealised rheologies, approximately mimicking the range between brittle failure of intact rock and frictional reactivation of pre-existing fractures, are used to calculate the FP (Table 1). The FE results contain the stress and strain tensors at each element integration point and the displacements at each node. The differential stress, mean stress and stress orientations are derived directly from the modelled stress tensor. The idealised rheologies include cohesion (C_0; assumed to be twice the tensile strength (Price & Cosgrove, 1990)), and the coefficient of friction, μ. The FP is calculated at each integration point using the stress data and these two parameters.

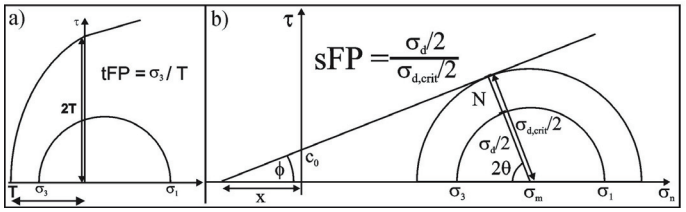

Figure 2. Mohr diagrams illustrating the fracture potential concept.
a) In the tensile regime ($\sigma_d < 4T$) tFP is the ratio between s3 and T, and is negative by convention. At tensile failure (s3 = -T) and tFP = -1. When s3 > 0 tensile failure is not possible and tFP = 0.
b) In the shear regime ($\sigma_d > 4T$) sFP is the ratio between the critical differential stress at failure $\sigma_{d,crit}$ and the observed differential stress σ_d.

Post-processing rheology_1 mimics intact rock with μ being the coefficient of internal friction and C_0 being the average value of intact cohesion for granitic plutons (Landolt-Börnstein, 1982). Post-processing rheology_7 mimics the reactivation of pre-existing faults, with μ in this case being the coefficient of sliding friction and C_0 the fracture strength. This was the weakest rheology considered since the maximum differential stress magnitudes in all the models were typically in the 15-30MPa range and mean stresses were generally close to zero. Under these stress conditions shear failure occurs close to the τ axis of a Mohr diagram and is much more sensitive to C_0 (τ axis intercept) than to the μ (gradient of the failure envelope). Hence, μ wasn't decreased below 0.6.

Table 1. Post-processing' rheologies applied to all FE results. Rheology_1 mimics intact rock, with μ being the coefficient of internal friction and C_0 being intact cohesion as an average value for granitic plutons. Rheology_7 mimics the reactivation of pre-existing faults whereby μ is the coefficient of sliding friction and C_0 is the fracture cohesion.

Rheology	μ	C_0 [MPa]	Notes
1	1.43	22	Intact rock
2	1.2	15	:
3	1	10	:
4	1	5	:
5	0.8	10	:
6	0.8	5	:
7	0.6	2.2	reactivation of faults only

Results

Model Time Span

The temporal stress loading on the Coso Range was examined for periods of 1, 10, 50, 100 and 1000 years. The differential stresses generated for the 1 and 10 year periods are insufficient to generate the number of shear fractures observed

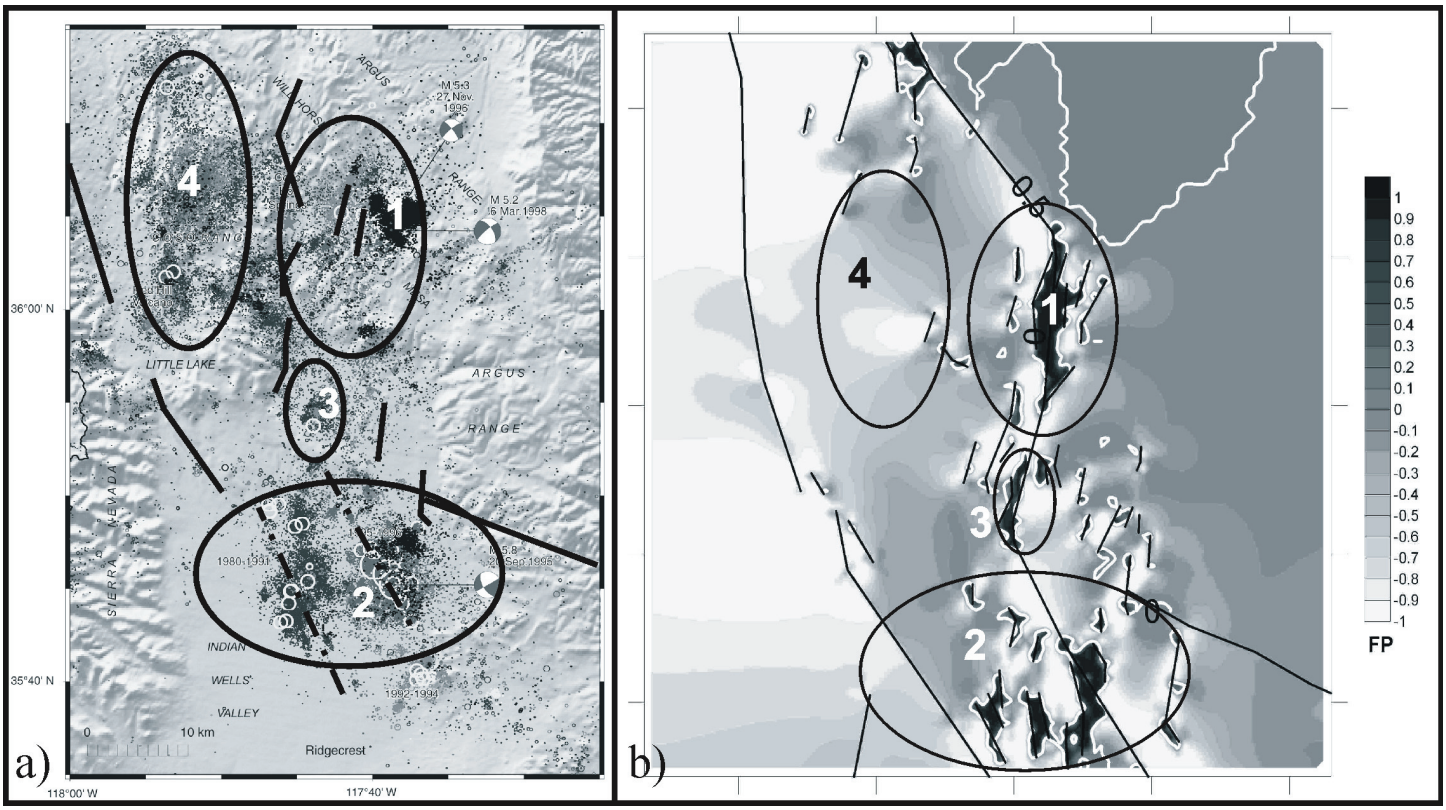

Figure 3. Earthquakes recorded by the Southern California Seismic Network between 1980 – 1998 (a) compared to regions of predicted shear fracturing from FE results for rheology_7 (b). Region (1) has a good fit predicting the overall dense seismicity, but does not include the seismic cluster of the 1996 and 1998 earthquakes. Regions (2) and (3) provide good matches to the observed seismicity. The large seismic area of Region (4) is not predicted to fail in shear, since the geometry used does not include the Cactus Flat Faults now known to be there.

in the seismicity data. Accumulated stress loading equivalent to 100-1000 years yields appropriately high differential stress magnitudes. However, these long periods are not considered realistic for a region as seismically active as Coso since stresses are likely to have been reduced by one or more major (>M5) earthquakes. The 50-year time step generates differential stresses sufficient for shear fractures to develop, and is an appropriate time span over which to model the unreleased stress loading in the Coso Range. Shear fractures are located along the bend structure and within the ALFZ (Figure 3).

Comparison of Fracture Potential Analysis and Seismicity

The 50 year FE modelling results were used to calculate the FP for each of the seven post-processing rheologies. Shear fracturing is predicted in multiple locations for all the post-processed rheologies (_1 to _7; Table 1). However, since the modelled differential stress magnitudes are relatively low, regions of shear fracturing with dimensions similar to the observed seismicity are not possible for the stronger rheologies. Thus, the analysis of the post-processed rheologies, in which rheology_7 provides the best fit to the observed seismic events (Figure 3), suggests that the main brittle deformation mechanism active in the study area is fracture reactivation. It is important to note that this FP analysis is applicable to the order of fractures below the second order faults included in the FE model. Using the current hierarchy, these fractures would be third order structures and have dimensions in the 100m to 1km range.

Many dextral strike-slip seismic events have occurred along the northern Coso Range (labelled 1 on Figure 3), and FP analysis using rheology_7 predicts a large number of shear fractures in the Northern Coso Range and suggests that the synthetic set would also fail dextrally. Unfortunately, the regions of the 1996 and 1998 earthquake clusters are not predicted to fail. In the Airport Lake Fault Zone a good correlation exists between the observed seismic activity and predicted shear fractures (labelled 2 on Figure 3). The seismic cluster at the southern end of the Coso Wash Fault also correlates very well to the rheology_7 results in both location and in spatial extent (labelled 3 on Figure 3). No correlation exists between the seismic cluster around the Cactus Flat fault (labelled 4 on Figure 3) in the west, and the predicted shear fractures. This occurs because the Cactus Flat Faults were not included in the FE model since they had not been identified when the base map used for the FE model was drawn. Since these structures have similar seismic signatures (i.e. are analogous) to the second order faults that have been modelled, they should behave in a similar way and the author's would expect the modelling to predict fractures in their vicinity. This emphasises the need to include all the faults (both main and second order) into the FE model.

Sierra Nevada Sensitivity Analysis

Regional scale FP results indicate that the motion applied to the Sierra Nevada Block is the most important loading condition affecting the region of the sub-model. A model series applying between 100% and 10% of the current Sierra Nevada motion (13mm/yr; Dixon et al., 2000) relative to stable North America was conducted. The aim of this model series was to determine the range of displacement magnitudes for which the FP magnitude suggests a transtensional regime (tFP in range –0.1 to –0.5) whilst generating strain orientations that match the strain observed pattern across the Coso Range.

In the 40%–100% models the tFP results adjacent to the Sierra Nevada Block are close or equal to –1, implying that the region is more likely to fail in tension than is observed. The modelled tFP values increase as the Sierra Nevada pull is reduced, such that models with <10%–40% lack the extreme tFP magnitudes and restricts regions of tFP = –1 to the extensional Sierra Nevada Frontal Fault and the Cactus Flat Faults (although the latter are not incorporated in the FE model). Models between 25 and 35% suggest that regions in the west where tensile failure is most likely (i.e. FP = -1) are spatially restricted to the trend of the Sierra Nevada Frontal Fault (Figure 3b). A transtensional regime, with tFP magnitudes between –0.2 to –0.5, is obtained within the bend structure. Only strain orientations from the >25% models have a good fit to those of Unruh et al. (2002 ; Figure 4).

Strain Orientations

Unruh et al. (2002) inferred the orientations of maximum incremental shortening and extension from kinematic inversions of earthquake focal mechanisms. These results are consistent with other studies (e.g. Gan et al., 2000) which concluded that Coso is located in a regime with maximum compression orientated ~NE- SW and maximum extension ~NW-SE.

The strain orientations obtained from the FE model are very similar to those of Unruh et al. (2002) and have a good fit to the NE- SW compression and NW-SE extension regime (Figure 4).

- The modelled direction of maximum shortening strain (~NE-SW) correlates well in the region close to the Sierra Nevada Frontal Fault (location 'A' in Figure 4).
- Strain directions in region 'B' on Figure 4 indicate a swing from NNE-SSW in the south of 'B' to ~NW-SE in the northern part. The FE results also show this swing, even though the modelled orientations, swinging from N-S in the south of 'B' to ~NW-SE in the north, are slightly different.
- Adjacent to the bend structure ('C' Figure 4), a 45° difference between the FE and seismic inversion directions exist. Unruh et al. (2002) obtained ~NNE-SSW orientations whereas the FE results predict ~NNW-SSE directions.
- The strain orientations in region 'D' on Figure 4 correlate well to the ~NE-SW direction of Unruh et al. (2002).
- At 'E' (Figure 4) the FE results show slight variations to the approximate N-S direction of Unruh et al. (2002).

The differences between the strain orientations in regions B, C and E on Figure 4 are most likely due to use of approximate fault slip magnitudes on the second order faults in the FE modelling whereas Unruh et al. (2002) used the complete earthquake focal mechanisms for their kinematic inversions. The strain orientations in the western part of the sub-model

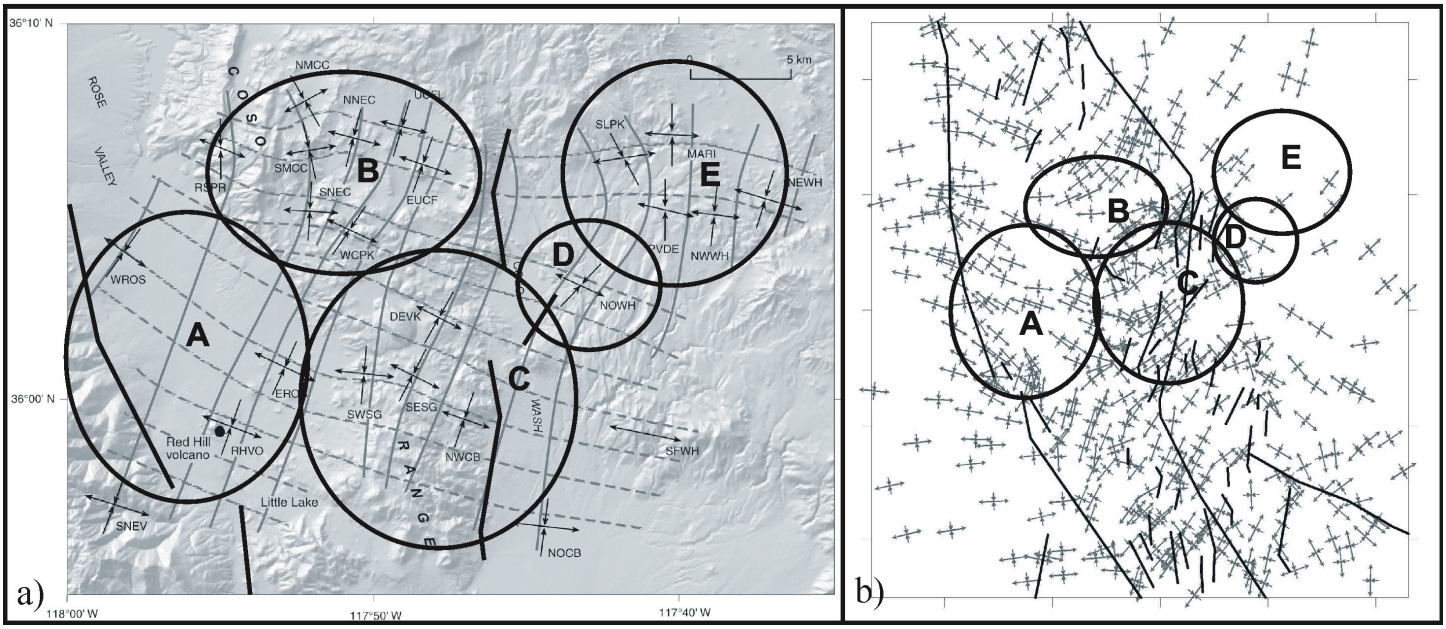

Figure 4. Comparison of the strain directions (a) obtained by Unruh et al. (2002) to the maximum shortening strain direction calculated for a FE model (b). 35% of the Sierra Nevada Block motion with respect to stable N. America was applied to this model. Best fits occur in regions (1) and (2) indicating the importance of the Sierra Nevada pull. Regions (3), (4) and (5) show minor differences (see text for details).

provide a better fit than elsewhere, emphasizing the critical influence of Sierra Nevada pull in generating the Coso Range transtensional system.

Summary and Conclusions

2D homogeneous linear elastic FE models of the ECSZ have been conducted in order to analyse the fracture networks expected in Coso Range and to provide external loading conditions for ongoing 3D FE models of the region.

Motion of the Sierra Nevada Block is the most critical loading condition for re-production of the transtensional regime observed in the Coso Range. A good fit is obtained for a relative displacement between the Sierra Nevada and Coso Range that is 25-35%, (i.e. 3.25-4.6mm/yr) of the total Sierra Nevada versus stable N. America motion.

The predicted synthetic shear and tensile fracture orientations correlate well to mapped fracture sets (e.g. White Horse Mesa), and ~normal to the maximum extensional strain orientation respectively. The technique of fracture potential suggests that deformation is predominantly occurring by reactivation of existing fractures and that the Coso Range can only be reliably modelled by incorporation of all second order structures. Furthermore, since a high degree of confidence can be placed on the 2D FE results it is possible to use them as the basis for local scale analysis of the fracture related fluid flow in the Coso Geothermal Field and for 3D FE models of the ECSZ and Coso Range.

Acknowledgments

We would like to thank the US Navy Geothermal Program Office (contract No. N68936-02-R-0235) for funding this work. Frank Monestero, Jeff Unruh, Tim Dooley and Ken McClay are thanked for useful discussions on Coso, the ECSZ and analogue modelling results.

References

ABAQUS User Manual: Version 6.3 (2003). Hibbitt, Karlsson & Sorensen, Inc.

Bennett, R.A., Wernicke, B.P., Davis, J.L., Elósegui, P., Snow, J.K., Abolins, J., House, M.A., Stirewalt, G.L. and Ferrill, D.A., 1997. "Global Positioning System constraints on fault slip rates in the Death Valley region, California and Nevada." Geophys. Res. Lett., Vol.24, No.23, p. 3073-3076.

Connolly, P.T., 1996, "Prediction of fluid pathways and secondary structures associated with dilational jogs." Unpubl. Ph.D thesis, Imperial College, London.

Connolly P.T. & Cosgrove, J.W., 1999. "Prediction of fracture induced permeability and fluid flow in the crust using experimental stress data." AAPG Bull. V.85, No.5, P. 757-777.

Dixon, T.H., Miller M., Farina F., Wang H. and Johnson D., 2000. "Present-day motion of the Sierra Nevada block and some tectonic implications for the Basin and Range province, North American Cordillera." Tectonics, 19, p. 1-24.

Dokka, R.K. and Travis C.J., 1990. "Role of the Eastern California shear zone in accommodating Pacific-North American plate motion." Geoph. Res. Lett., 17, p. 1323-1326.

Dooley, T., McClay, K. and Monastero, F.C., 2003 "Scaled sandbox modelling of transtensional pull-apart basins – applications to the Coso Geothermal System." Proceedings of the Eighth Annual Geothermal Program Office Technical Symposium, Davis, Ca.

Duffield, A.W., Bacon, C.R. and Dalrymple, G.B., 1980. "Late Cenozoic volcanism, geochronology, and structure of the Coso Range, Inyo County, California." J. Geophys. Res., 85, p. 2381-2404.

Feng, Q. and Lees, J.M., 1998. "Microseismicity, stress, and fracture in the Coso geothermal field, California." Tectonophysics 289, p.221-238.

Gan, W., Svarc, J.L., Savage, J.C., and Prescott, W.H., 2000. "Strain accumulation across the Eastern California Shear Zone at latitude 36°30'N." J. Geophys. Res., 105, No. B7, p.16229-16236.

Jaeger, J.C., and Cook, N.G.W., 1969. "Fundamentals of rock mechanics." Chapman and Hall LTD and Science Paperbacks.

Landolt-Börnstein V/1, 1982. "Physical properties of rocks." Springer Verlag, Berlin.

McClusky, S.C., Bjornstad, S.C., Hager, B.H., King, R.W., Meade, B.J., Miller, M.M., Monastero, F.C. and Souter, B.J., 2001. "Present-day kinematics of the Eastern California Shears Zone from a geodetically constrained block model." Geophys. Res. Lett., Vol. 28, No. 17, p. 3369-3372.

Monastero, F.C., Walker, J.D., Katzenstein, A.M. and Sabin A.E., 2002. "Neogene evolution of the Indian Wells Valley, east-central California." Geological Society of America, Memoir 195, p.199-228.

Price, N.J. & Cosgrove, J.W., 1990. "Analysis of geological structures." Cambridge University Press, Cambridge. pp502.

Roquemore, G.R., 1980. "Structure, tectonics, and stress field of the Coso Range, Inyo County, California." J. Geophys. Res., 85, p. 2434-2440.

Turcotte, D.L. & Schubert, G., 2002. "Geodynamics." Cambridge University Press, Cambridge. pp347.

Unruh, J.R., Hauksson, E., Monastero, F.C., Twiss, R.J. and Lewis, J.C., 2002. "Seismotectonics of the Coso-Indian Wells Valley region, California: Transtensional deformation along the southeastern margin of the Sierran microplate." Geological Society of America, Memoir 195, p. 277-298.

Walter, A.W., and Weaver, C. S., 1980. "Seismicity of the Coso Range." J. Geophys. Res., 85, p. 2441-2458.